Structural Growth and Viscoelastic Properties of Adsorbed Alginate Layers in Monovalent and Divalent Salts

Alexis J. de Kerchove and Menachem Elimelech*

Department of Chemical Engineering, Environmental Engineering Program, Yale University, P.O. Box 208286, New Haven, Connecticut 06520-8286

Received December 28, 2005; Revised Manuscript Received July 7, 2006

ABSTRACT: The growth and evolution of the viscoelastic properties of an alginate layer as a function of ionic strength and the presence of divalent calcium ions are monitored by quartz crystal microbalance with dissipation and atomic force microscopy. The properties of the alginate layer are investigated by combining results of incremental layer thickness or adsorbed areal mass, viscoelastic properties of the film, adhesion forces between adsorbing polysaccharides, and pull-off distances of the adsorbed molecules. In the absence of calcium, alginate adsorption behavior is strongly influenced by charge screening of the negatively charged carboxyl moieties of the alginate molecules. Reduction in alginate layer swelling is observed as ionic strength is increased, most likely due to Donnan equilibrium effects. The presence of calcium ions induces the formation of a thick and fluid gel layer via the complexation of alginate molecules. As the monovalent salt concentration is increased, a displacement of the ion-exchange equilibrium takes place in response to the competition between monovalent (potassium) and divalent (calcium) cations. The resulting impact of this phenomenon on the structure and viscoelastic properties of the alginate layer is discussed.

1. Introduction

Alginates are unbranched polysaccharides produced by brown algae as the principal component of their cell wall.[1,2] Alginates are also produced by Gram-negative bacteria,[3] such as *Pseudomonas aeruginosa*, and play an important role in the cohesion and protection of the microorganism in biofilm matrixes.[4] Commercially extracted alginates find broad applications in various fields that require the ability to control the structure of biological products, such as in the food,[5] textile,[6] and biomedical industries.[7] Adsorption and accumulation of alginate cause the fouling of engineered and biomedical devices that are contaminated by alginate-producing bacteria.[8−10]

Alginates have unique chemical and physiochemical properties, influenced by their composition and the solution chemistry of their surrounding environment. These polyelectrolytes are made of pattern blocks of homopolymeric regions of two residues: mannuronic (M) and guluronic (G) acids.[11] The M and G monomers have respective pK_a values of 3.38 and 3.65, rendering them negatively charged at near neutral pH. The specific conformation of the guluronic acid region allows the preferential electrostatic sequestration of divalent cations, such as calcium, at a yield of 3 cations for 12 sugar monomers. The complexation of the alginate molecules in the presence of calcium allows the formation of gel structures of various densities and is a function of the relative proportion and distribution of the M and G residues.[12] This controllable nature of alginates makes them valuable polymers for preparing materials with controlled structure and density.

The evolution of the structural properties of alginate layers, such as the viscoelasticity and intermolecular forces, under various solution chemistries, is highly dependent on the ionic composition of the surrounding solution.[13] However, conformational changes of the growing layer as new macromolecules adsorb under different ionic compositions are not well understood. The specific chemical and physical properties of alginates create major difficulties in understanding variations in the nature of inter- and intramolecular associations. The high negative charge of alginates due to the deprotonated carboxylic functional groups at near neutral pH induces repulsive inter- and intramolecular electrostatic forces. Alginate stability in solution is also maintained by steric repulsion between the macromolecules.[14] These interactions, which are a function of the conformation of the polysaccharide, are governed by the hydration of the molecules, the magnitude of the intramolecular electrostatic forces, the formation of hydrogen bonds and cationic bridges, and the M/G ratio. Changes in conformation affect the stability of the molecules not only in solution but also in the adsorbed state at the solid−liquid interface.

The quartz crystal microbalance with dissipation (QCM-D) is a useful tool to study the adsorption of macromolecules, such as polysaccharides, on a substrate in situ, in real time, as a function of solution chemistry.[15] The principles of this instrument have been extensively described.[16] The associated monitoring of shifts in frequency and losses of energy (also introduced as dissipation shifts) of the piezoelectric quartz as materials adsorb on its surface enables analysis of the viscoelastic properties of the deposited film.[17] The variation of the film thickness and the changes in shear viscosity and elastic shear modulus of the film provide information about the structure of the adsorbed macromolecules and the water that is associated with them.

The atomic force microscope (AFM) is an important tool commonly used to study the interaction forces between adsorbed materials at the solid interface and suspended macromolecules in solution, simulated by a colloidal probe.[18] Adhesion forces and interaction energies between adsorbed macromolecules can be determined at specific chemical conditions. Such force curves provide information about the local properties of the polymers, including their elasticity, charge density, hydration state, and adhesion.[19,20] AFM measurements can be combined with and complement the viscoelastic measurements obtained by QCM-D for investigating adsorbed macromolecule layers.[21]

* Corresponding author: phone (203) 432-2789; fax (203) 432-2881; e-mail menachem.elimelech@yale.edu.

10.1021/ma0527606 CCC: $33.50
Published on Web 08/24/2006

The main objective of this paper is to combine the use of these two tools, the QCM-D and AFM, to study the growth and evolution of viscoelastic properties of an adsorbed alginate layer as a function of the ionic composition of the electrolyte solution. Results are related to the inter- and intramolecular interactions between alginate macromolecules in solution and alginates adsorbed at the solid interface. Special emphasis is placed on the impact of divalent calcium ions on the adsorption and changes in conformation of the adsorbed polysaccharide layer.

2. Materials and Methods

2.1. Alginate Macromolecules and Solution Chemistry. Sodium alginate derived from the alga *Macrocistys pyrifera* was obtained from Sigma (St. Louis, MO). Alginates are linear unbranched polymers containing β-(1→4)-linked D-mannuronic acid and α-(1→4)-linked L-guluronic acid arranged in blocks of similar residues. The percentage of mannuronic and guluronic blocks is respectively 38 and 62%. The number-average molecular mass is 72.7 kDa, and its degree of polymerization is 367. Sodium alginate was dissolved in deionized water (Barnstead), and the stock solution (2 g/L) was stored at 4 °C. The final alginate concentration used in the adsorption experiments was 0.1 g/L, achieved by diluting the stock solution in the electrolyte solution of interest at ambient pH (5.5−5.7). The mannuronate and guluronate pK_a values are 3.38 and 3.65, respectively, rendering the alginate macromolecules negatively charged at the ambient experimental conditions (pH 5.5−5.7). The viscosity of the alginate solution was measured with an AR 2000 stress-controlled rheometer (TA Instruments, New Castle, DE) over a wide range of salt concentrations to be used in the adsorption experiments (described later).

All electrolyte solutions were prepared in deionized water with reagent-grade salts (Fisher) and stored at 4 °C. Effects of ionic strength on alginate adsorption were studied by adding a monovalent electrolyte (KCl) at concentrations ranging from 3 to 300 mM. To study the impact of calcium ions on alginate adsorption, 1 mM $CaCl_2$ was added to the electrolyte (KCl) solution of interest. The alginate stock solution was added to the electrolyte solution immediately prior to the adsorption experiments.

2.2. Model Surface for Adsorption Studies. AT-cut quartz crystals, supplied by Q-sense AB (Gothenburg, Sweden), were used. The crystals have a thickness of 0.3 mm, a fundamental frequency $f_0 \approx 5$ MHz, and a sensitivity constant of 0.177 mg m^{-2} Hz^{-1}. The crystals were supplied with silica (SiO_2) coating formed by vapor deposition. The silica substrate has a point of zero charge near pH 3.0 and is thus negatively charged during the adsorption experiments.[22] For AFM studies, the substrate used was a 10 mm × 10 mm quartz microscope slide (Electron Microscopy Science, WA) of 1 mm thickness. Both surfaces were cleaned for a minimum of 4 h in a 2% Hellmanex II solution (Hellma GmbH & Co. KG, Müllheim, Germany) at 50 °C, rinsed thoroughly with deionized water, and oxidized for 15 min in an UV/O_3 chamber.

Initial alginate adsorption onto the silica surface was made favorable by adsorbing a conditioning layer of poly-L-lysine (PLL) on the silica or quartz surface. Poly-L-lysine hydrobromide (Sigma) was used. Cationic PLLs have a molecular weight ranging from 70 to 150 kDa. PLL was dissolved in HEPES buffer (pH 7.4) made from 10 mM *N*-(2-hydroxyethyl)piperazine-*N*′-2-ethanesulfonic acid (Sigma), 100 mM KCl, and deionized water and stored at 4 °C. The final concentration of the stock PLL solution was 0.4 g/L. QCM-D results showed that an exposure of the SiO_2 substrate surface to the PLL stock solution for 15 min was enough to create a homogeneous layer. The conditioning PLL film was rinsed three times for 15 min with the electrolyte solution used for the subsequent first alginate adsorption experiment.

2.3. QCM-D. Alginate adsorption and adsorbed layer properties were studied using a quartz crystal microbalance with dissipation (QCM-D) instrument (Q-Sense D300, Q-Sense AB, Gothenburg, Sweden). Shifts in frequency and dissipation are measured at three overtone frequencies ($n = 3$, 5, and 7) as the materials adsorb onto the quartz surface, allowing the calculation of the thickness and viscoelastic properties of the adsorbed film. In this work, the interpretation of viscoelastic properties of the adsorbed film was based on the model presented by Voinova et al.[23] The adsorbed hydrated layer was considered as a single Voigt element with given shear viscosity and elastic shear modulus. Further, the quartz was assumed to be purely elastic, and the surrounding solution was considered to be viscous and Newtonian. The density and viscosity of the liquid used in the model were respectively 1000 kg/m^3 and 0.001 Pa·s. The thickness and the density of the adsorbed film were considered uniform. As the value of the film density has only a minor impact on the fitted results,[21] a film density of 1030 kg/m^3 was used in all computations. It was also assumed that the viscoelastic properties were frequency-independent and that there was no slip between the adsorbed molecules and the crystal during shearing.

Results from measurements were fitted to this model using the program Q-Tools provided by Q-Sense AB. The data sets recorded with harmonics 3, 5, and 7 were used to compute and confirm the best fitting of the thickness or areal mass, the shear viscosity, and the elastic shear modulus of the adsorbed layer. Results obtained by the four possible combinations of the data sets (with the three harmonics) provided similar iterations for the three unknowns.

2.4. Intermolecular Force Measurements. Atomic force microscopy (AFM) was used to measure the adhesion forces between alginate in solution and alginate in the adsorbed layer as the ionic composition of the bulk solution varied. Because carboxylic groups are the predominant functional groups of alginate, a carboxylated modified latex (CML) particle (Interfacial Dynamic Corp., Portland, OR) was used as a surrogate for alginate. The CML particle (4 μm in diameter) is covered with a porous and highly charged polyelectrolyte layer, rich in carboxylated groups, with a titrated surface charge of 139.5 μC/cm^2. A colloid probe was made by attaching the particle to a tipless SiN cantilever (Veeco Metrology Group, Santa Barbara, CA) with a spring constant of 0.06 N/m. A drop of CML colloidal suspension was first spread on a freshly cleaved mica surface and dried with an Ar gas. Using a laboratory fabricated micromanipulator, a small amount of glue (Norland Optical Adhesive, Norland Products, Inc., Cranbury, NJ) was spread on the free end of the tipless SiN probe. A single CML particle was then attached to the cantilever end, with only a small surface area of the particle in contact with the glue. The glue was cured for 15 min under UV. The strength of the colloid probe was tested by applying forces to the attached particle from different angles using another unmodified cantilever. A new colloid probe was used for each experiment. The probes were carefully examined before and after their use to ensure their integrity.

Force measurements were conducted in a fluid cell with closed input and output. Solution conditions tested were similar to those used in the QCM-D adsorption experiments. A minimum of 6 mL for each solution was injected into the cell when a change of the solution chemistry was induced. Because of local surface heterogeneities, force measurements were performed at five different locations, with a minimum of 10 replicates at each location.

Adhesion forces were obtained by operating the AFM in contact mode. The raw data, that is, cantilever deflection vs cantilever displacement, were first processed to remove optical interferences. The resulting curves were then converted to force normalized by the colloid probe radius vs surface-to-surface separation curves using the method reported by Ducker et al.[24] From each coherent force curve, the maximum adhesion force, the integrated adhesion force (i.e., interaction energy), and the maximum pull-off distance were extracted. Averages of these parameters and standard errors were calculated considering a 90% confidence interval.

2.5. Alginate Adsorption Protocol and Result Analysis. QCM-D and AFM were used to study alginate adsorption mechanisms. When injecting the electrolyte and alginate solutions to the QCM-D and AFM cells, the flow is horizontally radial for the QCM-D and parallel to the quartz surface in the case of the AFM liquid cell. Because both systems are used in batch mode, the difference in geometry and resulting hydrodynamics have a minimal

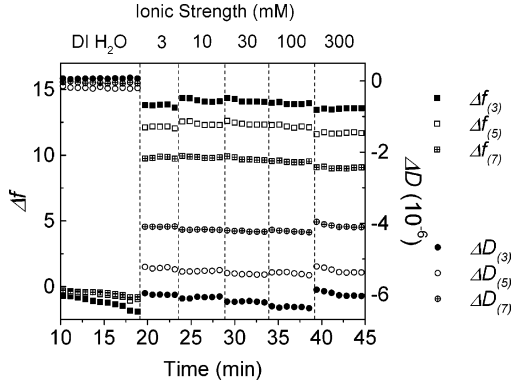

Figure 1. Effect of transitions in electrolyte concentration on the three resonance frequencies ($\Delta f_{(3)}$, $\Delta f_{(5)}$, and $\Delta f_{(7)}$) of the QCM-D quartz and the corresponding dissipations ($\Delta D_{(3)}$, $\Delta D_{(5)}$, and $\Delta D_{(7)}$). The batch QCM-D experiment is run on a bare SiO_2 surface, varying the KCl concentration in solution from 0 to 300 mM at an ambient pH.

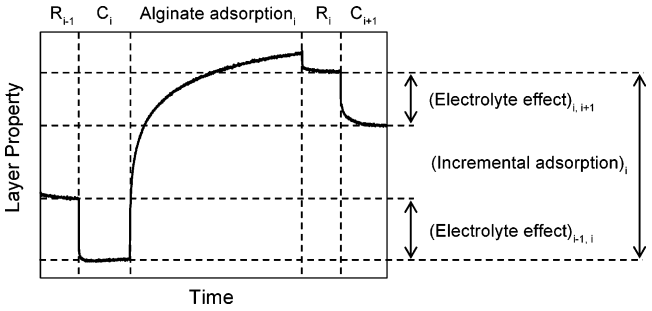

Figure 2. Delimitation of the conditioning (C_i), alginate adsorption, and rinse (R_i) at a specific ionic strength (i) and definition of the specific variations of the layer property in response to the electrolyte effect and to the incremental adsorption. The plot is based on a representative QCM-D experiment and illustrates the variation in the layer property over time as a function of the various steps in the experiment described in the text.

effect on alginate adsorption. Ionic strength was increased incrementally during the course of an experiment by replacing the electrolyte solution filling the QCM-D chamber or AFM liquid cell. As shown in Figure 1, it was verified that these transitions between the different alginate-free solutions did not induce significant frequency and dissipation shifts of the bare quartz of the QCM-D. A first layer of alginate was adsorbed onto the PLL layer for 15 min, responding to PLL−alginate interactions. To study alginate−alginate interactions, consecutive alginate layers were adsorbed on top of the initial PLL−alginate layer with the ionic strength, IS_i, increasing incrementally. The index i goes from 1 to 5 and corresponds to a specific ionic strength within the studied ionic strength range. The adsorption of these layers was obtained by following a three-step protocol as depicted in Figure 2. For each ionic strength, i, the procedure started with the replacement of the IS_{i-1} solution with the electrolyte solution IS_i and the conditioning, C_i, of the present adsorbed layer with the new electrolyte solution for 15 min. Following the conditioning step, alginate solution at IS_i was injected into the system to adsorb and form a new layer, L_i, superposing layer L_{i-1}. Adsorption took place for 15−90 min until the measured shifts in frequency and dissipation would be insignificant. The last step was the rinse, R_i, of the alginate layer with the electrolyte solution IS_i to remove alginate in solution and to allow the relaxation of the newly adsorbed layer for 15 min. A new batch adsorption cycle at IS_{i+1} was started after this last step.

Two different types of information were extracted from the collected data. As shown in Figure 2, the impact of the transition in ionic strength from IS_{i-1} to IS_i (or from IS_i to IS_{i+1}) on the layer properties was determined as being the difference in property value between C_i and R_{i-1} (or between C_{i+1} and R_i). It was called the "electrolyte effect" at IS_i (or IS_{i+1}). The direct impact of alginate adsorption during step L_i on the total layer properties was also

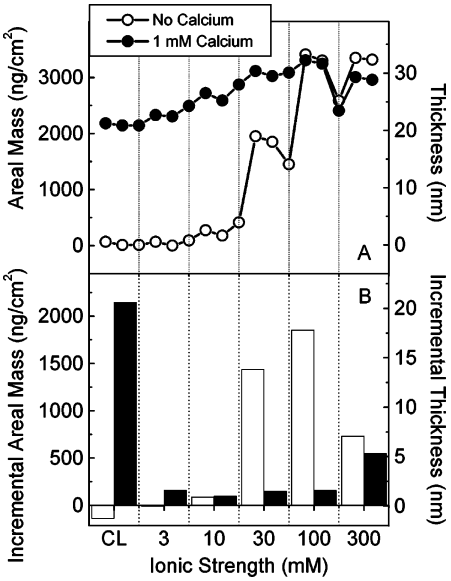

Figure 3. (A) Evolution of the thickness of the adsorbed alginate layer and (B) incremental variation of the thickness following alginate adsorption obtained by QCM-D as a function of ionic composition. The variations in thickness of the layer can also be interpreted as variation in areal mass considering a fixed layer density of 1030 kg/m^3. The increments in thickness of the adsorbed layer in the absence (open bars) and presence of calcium (black bars) are measured for the conditioning layer (CL) of alginate on the PLL layer at 3 mM ionic strength and for the successive alginate layers adsorbed at increasing ionic strengths from 3 to 300 mM. The increments are calculated by the difference in measured thickness observed between the rinse of the freshly adsorbed alginate and the conditioning of the existing layer. For the first layer shown (CL), the increment is calculated as the difference between the second data point and the conditioning of the PLL layer with no alginate (data is not shown). The best fittings for this parameter are obtained considering the harmonics 3, 5, and 7 using the Voigt-based model considering a single-layer system.

calculated by the difference in property values between R_i and C_i at the same ionic strength. This layer property was called the "incremental adsorption" at IS_i. The results obtained for the electrolyte effect as a function of ionic composition were 1−2 orders of magnitude smaller than the results of the incremental adsorption. For this reason, the electrolyte effect is not shown or discussed in this work.

3. Results and Discussion

QCM-D and AFM results are combined to study the growth and evolution of viscoelastic properties of the adsorbed alginate layer as a function of the ionic composition of the background solution. Specific information about the structure of the layer and alginate molecule conformation is extracted from four independent sets of results: (i) the thickness (or areal mass) of the layer, (ii) the intermolecular adhesion forces, (iii) the viscoelastic properties of the layer, and (iv) the pull-off distance of the adsorbed alginate molecules. The impacts of the presence of divalent calcium cations and of increasing ionic strength during the layer growth on the adsorbed layer properties are distinguished by analysis of these results.

3.1. Growth of Adsorbed Alginate Layer. The variation in thickness or areal mass of the adsorbed alginate layer as a function of ionic strength, obtained from the QCM-D data, is presented in Figure 3. The global changes in the layer thickness are seen in Figure 3a. For the first conditioning layer (CL) of alginate on the PLL, the first two data points are for alginate adsorption and layer rinsing with the background electrolyte; the conditioning of the PLL layer is not shown. The thickness (and areal mass) were offset at zero after the rinse of the PLL

layer. For each subsequent condition, three measurements are shown, corresponding to the conditioning of the existing layer, the adsorption of alginate, and the rinse of the layer with the background solution. The incremental variation of the layer property is extracted (Figure 3b) from the measurements obtained before and after the alginate adsorption at each condition.

In the absence of calcium, adsorption of alginate onto the PLL layer induces a decrease in the incremental thickness. The very strong alginate−PLL electrostatic attraction favors the adsorption of alginate to the PLL layer. The close interaction between the two oppositely charged polyelectrolytes causes the compaction of the resulting layer by expulsion of the water that was associated with the PLL molecules initially adsorbed on the quartz.[17] The addition of macromolecules and the related expulsion of water from the adsorbed layer result in the negative incremental thickness. The following additions of alginate to the layer with increasing ionic strength are insignificant until a total ionic strength of 30 mM is reached. Above 10 mM ionic strength, mass is successively added to the adsorbed layer. The increases in ionic strength induce charge screening of the negatively charged alginate macromolecules.[25] The absence of a direct relationship between the thickness (or areal mass) increments and the concomitant increases in ionic strength may be attributed to the presence of water molecules and salt ions associated with the adsorbing alginate macromolecules.

In the presence of 1 mM calcium ions in solution, the formation of the alginate layer and its growth with increasing ionic strength show major differences compared to the growth of the alginate layer in the absence of calcium, as seen in Figure 3a. The initial positive adsorption of alginate on the PLL layer at low ionic strength is significant and produces a precipitous increase in the layer thickness. Under these conditions, the adsorption of alginate is favored by the formation of gel structures induced by complexation of the alginate macromolecules with the divalent calcium cations.[26] Thus, the high layer thickness results from the favorable adsorption of polymer aggregates and water molecules onto the PLL layer. After its initial increase, the thickness increases by small increments as the ionic strength increases (Figure 3b). This incremental thickness is more significant at high ionic strength (300 mM) and is comparable in magnitude to the incremental thickness obtained at the same ionic strength in the absence of calcium. A mechanistic explanation for this behavior will be given later in this paper.

3.2. Intermolecular Interaction Forces. Intermolecular adhesion forces (Figure 4) were determined by the AFM colloid probe for ionic compositions similar to those used earlier in the QCM-D studies. Adhesion force measurements were taken prior to adsorption of additional polysaccharides onto the existing layer. Normalized forces between the colloidal probe and the precoated PLL layer are not shown in Figure 4 because of their very high magnitude. These PLL−alginate adhesion forces reached magnitudes of -3.9 ± 0.2 and -6.8 ± 0.1 mN/m in the absence and presence of calcium, respectively, indicating a strong electrostatic attraction between the positively charged PLL layer and the negatively charged alginates.

In the absence of calcium, the adhesion forces between the adsorbed alginates generally increase as the ionic strength increases. Specifically, above 10 mM KCl, the adhesion force becomes more significant as the ionic strength is raised. This increase in adhesion force corresponds to the reduction in electrosteric repulsion between the alginate molecules.[27] Consequently, we can confirm that the absence of correlation

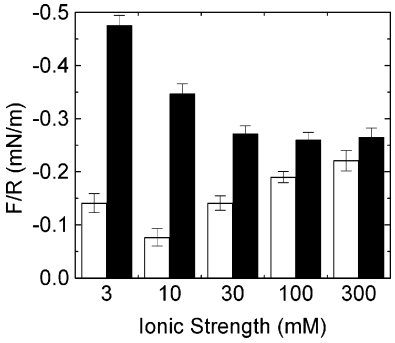

Figure 4. Variation of adhesion forces between the alginate-coated AFM colloidal probe and the existing adsorbed alginate as a function of the solution ionic composition. Adhesion forces are determined from the retraction of the probe from the surface prior to the alginate adsorption step of the experiment. Adhesion forces are normalized by the radius of the colloidal probe (F/R). The presented adhesion forces are for the absence (open bars) and presence of calcium ions in solution (solid bars). Error bars represent standard errors.

observed earlier in Figure 3 between the incremental variation in thickness (or areal mass) and ionic strength is related to the variation of the amount of water and salt associated with the adsorbed layer.

In the presence of calcium, the intermolecular adhesion forces are much more pronounced than those observed in the absence of calcium, and their evolution with increasing salt (KCl) concentration is not similar to that observed in the absence of calcium. At low ionic concentration, the normalized adhesion force is large, reaching up to 4.5 times the adhesion force measured between alginates in the absence of calcium. Such adhesion forces are attributed to the strong bonds formed between the negatively charged sites of the guluronate molecules constituting the alginate macromolecules by sequestration of calcium ions. These results verify our previous data on the incremental thickness of the layer by confirming the complexation of the polysaccharides and the formation of gel structures in the presence of calcium. As the ionic strength is increased, the adhesion forces decrease and reach a constant value above 30 mM ionic strength. This trend indicates that the strength of the bonds between the polysaccharides decreases as the concentration of the monovalent (KCl) salt in solution increases. This behavior suggests that there exists a strong competition between the monovalent and divalent cations for the binding sites on the polyelectrolytes.[28]

3.3. Viscoelastic Properties of Adsorbed Layer. The viscoelastic properties of the adsorbed alginate layer are determined by studying the relationships between the shifts in dissipation (ΔD) and the shifts in frequency ($\Delta f_{(n)}$) obtained by the QCM-D. The shifts in dissipation with decreasing frequency during alginate adsorption were studied as a function of ionic composition, using harmonic 3 (15 MHz). For each ionic composition, a linear relationship was observed between ΔD and $\Delta f_{(3)}$ during the alginate adsorption onto the substrate. Figure 5a shows representative dissipation shifts obtained during alginate adsorption in the absence of calcium. Each linear correlation corresponds to the data obtained between the end of the conditioning period and the start of the rinsing period. The ranges of ΔD and $\Delta f_{(3)}$ obtained for a specific ionic strength depend therefore on the adsorption capacity of the existing layer. Linear relationships were also obtained during alginate adsorption in the presence of 1 mM calcium (data not shown). The slopes of the linear relationship between ΔD and $\Delta f_{(3)}$ for each ionic composition are shown in Figure 5b.

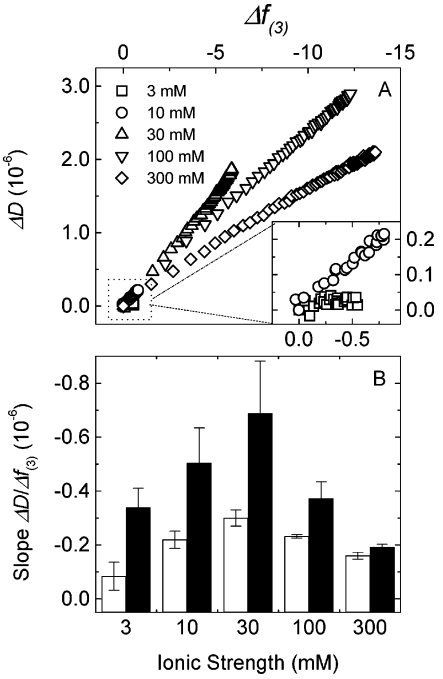

Figure 5. Estimation of the variation in dissipation as a function of frequency shift during the alginate adsorption phase. (A) Dissipation shift vs frequency shift plots using QCM-D data for harmonic 3. (B) Calculated slopes (dissipation shift/frequency shift) as a function of ionic strength and calcium presence (open bars = no calcium, solid bars = 1 mM Ca^{2+}). Error bars represent standard errors.

Considering that the losses in energy causing the damping of the quartz vibration are caused by the viscoelasticity of the layer adsorbed on the quartz, the slope $\Delta D/\Delta f_{(3)}$ gives the magnitude of the variations in the alginate layer viscoelasticity.[29,30] The trends observed for the change in slopes are confirmed with the fitted values of the elastic shear modulus and shear viscosity of the adsorbed layer calculated using the QTools software of the QCM-D. The variations in these two parameters are calculated for each ionic composition and are shown in Table 1. These variations in shear modulus and viscosity are informative of the change in viscoelastic properties of the layer during its growth by alginate adsorption.

In the absence of divalent cations, the slopes $\Delta D/\Delta f_{(3)}$ are all positive and increase in magnitude with increasing ionic strength to reach a maximum value at 30 mM KCl. At higher ionic strength, the variations in viscoelasticity decrease in magnitude. These variations in magnitude as a function of the salt concentration suggest that alginate adsorption on the existing layer causes either larger or smaller variations in viscoelasticity, depending on the ionic strength. At low ionic strength, the increase in viscoelasticity is small, revealed by low losses in energy, and suggests that the layer is rigid with a low water content, and stays compact despite the addition of mass on the quartz. Table 1 shows that the elastic shear modulus and shear viscosity at 3 mM KCl are the largest compared to values calculated at other ionic strengths. These values characterize a more rigid state of the layer after alginate adsorption. At intermediate ionic strength (30 mM KCl), the slope $\Delta D/\Delta f_{(3)}$ is the largest, indicating that incremental alginate adsorption on the quartz makes the layer more fluid by increasing the water content of the layer. This results in the reduction of the layer shear modulus and viscosity, as shown in Table 1. At higher ionic strength (300 mM KCl), the variations in viscoelasticity of the layer decrease in magnitude. The adsorbed alginates form a compact and rigid layer sequestering a small amount of water, as also suggested by the successive increases in shear modulus and viscosity shown in Table 1. Variations in viscoelastic properties of other macromolecules have been shown to be directly related to the change in the content of water associated with the molecules by hydrogen bonding.[17]

In the presence of calcium, the changes in the $\Delta D/\Delta f_{(3)}$ slopes reach larger magnitudes than those measured for the layer grown in the absence of calcium (Figure 3b). These larger losses in energy, indicative of the significant fluidity of the layer, are responses to the higher amount of water trapped in the adsorbed gel matrix.[17] Values of the elastic shear modulus and shear viscosity show a comparable trend in their shifts as a function of ionic strength, as shown in Table 1. The results suggest that the hydration of the layer changes with increasing ionic strength. The highest fluidity of the layer is reached at 30 mM KCl. At the highest salt concentration (300 mM), the adsorption of the alginate complexes forms a compact layer that seems to reach levels of energy loss similar to the losses obtained in the absence of calcium.

3.4. Pull-Off Distance of Adsorbed Alginate Molecules. The pull-off distance of the adsorbed alginate molecules is defined as the extension distance characterizing the stretching-out of the adsorbed alginate molecules or complexes during the retraction of the colloidal probe in our AFM experiments.[31,32] The pull-off distances are calculated from two independent variables: (i) the maximum value of the adhesion force and (ii) the normalized energy resulting from the integration of the adhesion force. We assume that the detachment of the alginate from the colloidal probe during its retraction from the surface occurs in a single pull-off event. The pull-off is modeled as the length of the side orthogonal to the maximum value of the adhesion force in a triangular-shaped adhesion force curve. The pull-off distances determined from the force measurements obtained after alginate adsorption are shown to vary as a function of the solution ionic composition, as depicted in Figure 6.

In the absence of calcium, the pull-off distance of the adsorbed alginate ranges from 68 to 81 nm, depending on solution ionic strength. The pull-off distance is reduced with increasing ionic strength, reaching a minimum value at a salt (KCl) concentration of 30 mM. At higher salt concentrations, the pull-off distance varies less significantly. These variations in pull-off distance suggest changes in the molecular conformation of the adsorbed alginate with increasing ionic strength. The polyelectrolytes transit from extended to coiled conformations as the negatively charged carboxyl moieties are screened by the monovalent potassium counterions.

Complexation of the alginate molecules in the presence of calcium has a significant impact on the variation of the pull-off distance with increasing ionic strength. The pull-off distances of the molecules increase by nearly constant increments, from 77 to 170 nm, as the ionic strength of the solution is raised to 100 mM. The initial pull-off distances at low ionic strength are significantly larger than the distances obtained in the absence of calcium at the same ionic strength, suggesting that complexes of alginate molecules can be extended further into solution than single molecules. The larger distances obtained at higher ionic strength in the presence of calcium suggest that the presence of higher concentrations of monovalent ions induces the alginate complexes to be less efficiently bound together. However, this reduction in complexation efficiency occurring at ionic strengths up to 100 mM does not result yet in the fractionation of the gel-like layer and allows complexed alginates to extend further into the solution during the AFM colloid probe retraction. At 300 mM ionic strength, the pull-off distance of the adsorbed alginates in the presence of calcium is reduced to a value similar

Table 1. Variations of Elastic Shear Modulus and Shear Viscosity of the Adsorbed Layer as a Function of the Solution Ionic Composition[a]

	absence of calcium		1 mM calcium	
ionic strength (mM KCl)	elastic shear modulus (10^3 N m^{-2})	shear viscosity (10^{-4} N s m^{-2})	elastic shear modulus (10^3 N m^{-2})	shear viscosity (10^{-4} N s m^{-2})
3	30.0	16.6	11.0	14.2
10	22.2	16.0	12.1	14.3
30	8.3	12.4	11.4	14.3
100	8.8	13.0	9.7	14.0
300	15.4	15.2	14.0	15.3

[a] These values of viscoelastic properties are calculated from the dissipation shifts measured during the rinse of the freshly adsorbed alginate layer at a specific ionic strength. The best fittings of these viscoelastic parameters are obtained using the Voigt-based model considering a single adsorbed layer with a fixed density of 1030 kg/m^3 in all cases.

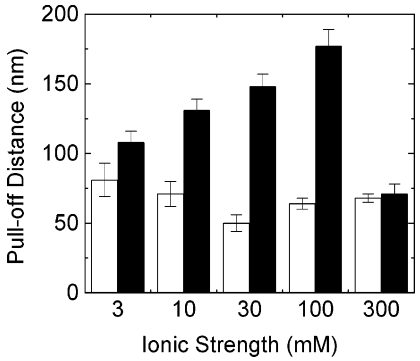

Figure 6. Variation of the pull-off distances of the adsorbed alginates using AFM data as a function of ionic strength, in the absence (open bars) and presence of 1 mM calcium (solid bars). Extension distances of the adsorbed molecules or complexes are calculated from the force measurements during the retraction and detachment of the colloidal probe from the surface after alginate adsorption. Error bars represent standard errors.

to the distance at the same ionic strength in the absence of calcium. This equivalence in the pull-off distances suggests that the complexation of alginate molecules by sequestration of calcium ions is significantly inhibited by the presence of monovalent salts. Thus, in this case the adsorbed alginate layer behaves as individual alginate molecules.

3.5. Adsorption and Alginate Layer Growth Mechanisms in Monovalent Salt. The QCM-D and AFM results presented earlier showed that alginate molecules can adsorb significantly on alginate films in the presence of monovalent salts. Inter- and intramolecular electrostatic interactions govern the adsorption of alginate molecules and therefore define the structure adopted by the growing layer. Our previous discussion also suggests that increasing ionic strength induces variations in the amount of water molecules sequestered in the inter- and intramolecular spaces of the polymer network that directly affect the swelling of the layer.[33] The complementary trends given by our results indicate that the adsorbed alginates adopt different molecular states with increasing ionic strength.

The increase in electrolyte concentration results in the compaction of the adsorbed layer and the increase of the polysaccharide adsorption. The reduction in the swelling of the alginate film at high ionic strength can be described as a response to the Donnan equilibrium. The adsorbed polyelectrolyte film acts as a semipermeable membrane with immobile charges distributed in its network and is subjected to a large concentration gradient induced by the mobile ions added in the surrounding solution.[34] Our results agree with previous reports on the reduction of volume of Na−alginate beads when the salt concentration in the external solution is increased.[35] This is in accordance with the Donnan equilibrium where the difference in ionic concentration between the inside of the film and the outside solution is reduced by displacement of the entrapped solvent (water) in response to the increase in the concentration of salt in the surrounding liquid.[36]

The electrostatic destabilization of the alginate molecules induces alginate adsorption by van der Waals interactions and the formation of hydrogen bonds. Under the pH condition examined (pH 5.5−5.7), most of the alginate molecules are entirely charged, although it is likely a small fraction of the carboxyl moieties of the polymer remain uncharged. These uncharged groups can form inter- and intramolecular hydrogen bonds that can contribute to the aggregation of the polysaccharides. Such electrostatic destabilization can also induce aggregation of alginate molecules in solution. However, we observed no phase separation in solution. Independent measurements of solution viscosity also confirmed this observation. The alginate solution has a constant viscosity of 0.0010 ± 0.0001 Pa·s at all studied ionic strengths, independent of the presence of calcium. The relatively low concentration of the alginate solutions used (0.1 g/L) and the reduced transport of suspended alginates in the quiescent batch system minimize the growth of large aggregates in solution. However, the constant depletion of alginates at the close vicinity of the layer due to adsorption favors mass transfer by diffusion from the bulk solution to the alginate layer. This diffusive transport allows bringing together suspended and adsorbed alginates. The reduction of the electrostatic repulsion forces helps the adsorption of transported alginate molecules by van der Waals forces and hydrogen bonding.

3.6. Adsorption and Layer Growth Mechanisms in the Presence of Divalent Calcium Ions. The AFM and QCM-D results reveal the marked influence of alginate complexation by calcium sequestration on the evolution of the adsorbed alginate layer as a function of ionic strength. The presence of 1 mM calcium induces the formation of a thick and highly viscoelastic gel layer by adsorption of alginate aggregates/complexes at the solid interface.[37] Results also demonstrate that increasing concentrations of monovalent ions in solution can cause the reduction and inhibition of alginate complexation by calcium. In the presence of monovalent counterions, an electrostatic competition takes place between divalent and monovalent salts for the negatively charged sites at the polysaccharide surface.[38] The ionic competition affects the potassium−calcium ion-exchange equilibrium by inducing progressive replacement of calcium ions by potassium ions.[39]

We have shown that a thick incremental gel layer adsorbs at low ionic strength. The results further illustrate that the high efficiency of calcium sequestration between coupled guluronate sequences forms strong bonds between the polymeric chains at multiple locations. The gel layer is more hydrated than the layer adsorbed without calcium, with water molecules trapped by hydrogen bonding in the gel matrix. As the monovalent salt concentration is increased (30 mM), the replacement of calcium ions by potassium ions reduces the degree of alginate complex-

ation and induces conformational changes of the gel matrix. Major swelling of the layer takes place in response to the ion-exchange process, and the gel matrix acts as a looser and more fluid structure. At the highest ionic strength (300 mM), the presence of calcium is overshadowed by the high potassium concentration. Consequently, the complexation of alginates in solution is inhibited. The gel matrix is partially dissolved by the progressive replacement of the calcium ions by potassium ions in the layer structure. In this case, the alginate molecules behave as in the case with no calcium and adsorb as individual molecules at the layer surface. The displacement of ion exchange equilibrium has been commonly observed for alginate fibers,[40] alginate gel beads complexed with calcium,[41] marine algal cell walls,[42] and alginate-coated particle aggregates in environmental and biomedical systems.[43,44] Such ion-exchange processes result in the swelling of the gel layer and the extension of the polymer network.

4. Conclusion

QCM-D and AFM are combined to study alginate adsorption from aqueous solutions and the evolution of the physicochemical properties of the resulting adsorbed layer. The QCM-D provides quantitative information on the film thickness on the silica surface as well as the viscoelastic properties of the adsorbed layer. The Voigt-based model used in the fitting of our results gives consistent information on the variations in thickness, elastic shear modulus, and shear viscosity of the viscoelastic layer. AFM is found to be a powerful complementary tool to interpret the evolution of the alginate layer properties obtained by QCM-D.

The QCM-D and the AFM data reveal a strong dependence between alginate adsorption and ionic strength, suggesting that electrostatic interactions play a paramount role in the control of layer structure. Our results confirm for the first time that the various impacts of concentrated salt solutions commonly observed for alginate bead structures, with or without calcium, also occur for adsorbed alginate layers. The swelling behaviors observed under various salt compositions are demonstrated by the correlations made between viscoelastic properties and interaction force measurements. Significant shifting of the potassium−calcium ion exchange equilibrium is also observed under the studied conditions.

Acknowledgment. Funding was provided by NSF Grant BES 0228911 and by the NSF Science and Technology Center for Advanced Materials for Purification of Water with Systems (CAMPwS). We thank Dr. Paul Van Tassel for use of the QCM-D.

References and Notes

(1) Davis, T. A.; Ramirez, M.; Mucci, A.; Larsen, B. *J. Appl. Phycol.* **2004**, *16*, 275−284.
(2) Andrade, L. R.; Salgado, L. T.; Farina, M.; Pereira, M. S.; Mourao, P. A. S.; Filho, G. M. A. *J. Struct. Biol.* **2004**, *145*, 216−225.
(3) Sutherland, I. W. *Int. Dairy J.* **2001**, *11*, 663−674.
(4) Korstgens, V.; Flemming, H. C.; Wingender, J.; Borchard, W. *Water Sci. Technol.* **2001**, *43*, 49−57.
(5) Brownlee, I. A.; Allen, A.; Pearson, J. P.; Dettmar, P. W.; Havler, M. E.; Atherton, M. R.; Onsoyen, E. *Crit. Rev. Food Sci. Nutr.* **2005**, *45*, 497−510.
(6) Rompp, W.; Beitlich, R. *Am. Dyest. Rep.* **1983**, *72*, 31−32.
(7) Uludag, H.; De Vos, P.; Tresco, P. A. *Adv. Drug Delivery Rev.* **2000**, *42*, 29−64.
(8) Pasmore, M.; Todd, P.; Smith, S.; Baker, D.; Silverstein, J.; Coons, D.; Bowman, C. N. *J. Membr. Sci.* **2001**, *194*, 15−32.
(9) Murga, R.; Miller, J. M.; Donlan, R. M. *J. Clin. Microbiol.* **2001**, *39*, 2294−2297.
(10) Sutherland, I. W. *Water Sci. Technol.* **2001**, *43*, 77−86.
(11) Schurks, N.; Wingender, J.; Flemming, H. C.; Mayer, C. *Int. J. Biol. Macromol.* **2002**, *30*, 105−111.
(12) Braccini, I.; Perez, S. *Biomacromolecules* **2001**, *2*, 1089−1096.
(13) Mancini, M.; Moresi, M.; Rancini, R. *J. Food Eng.* **1999**, *39*, 369−378.
(14) Rutland, M. W.; Senden, T. J. *Langmuir* **1993**, *9*, 412−418.
(15) Marx, K. A. *Biomacromolecules* **2003**, *4*, 1099−1120.
(16) Rodahl, M.; Hook, F.; Krozer, A.; Brzezinski, P.; Kasemo, B. *Rev. Sci. Instrum.* **1995**, *66*, 3924−3930.
(17) Hook, F.; Kasemo, B.; Nylander, T.; Fant, C.; Sott, K.; Elwing, H. *Anal. Chem.* **2001**, *73*, 5796−5804.
(18) Butt, H. J.; Cappella, B.; Kappl, M. *Surf. Sci. Rep.* **2005**, *59*, 1−152.
(19) Frank, B. P.; Belfort, G. *Langmuir* **1997**, *13*, 6234−6240.
(20) Frank, B. P.; Belfort, G. *J. Membr. Sci.* **2003**, *212*, 205−212.
(21) Gurdak, E.; Dupont-Gillain, C. C.; Booth, J.; Roberts, C.; Rouxhet, P. G. *Langmuir* **2005**, *21*, 10684−10692.
(22) Bourikas, K.; Kordulis, C.; Lycourghiotis, A. *Environ. Sci. Technol.* **2005**, *39*, 4100−4108.
(23) Voinova, M. V.; Rodahl, M.; Jonson, M.; Kasemo, B. *Phys. Scr.* **1999**, *59*, 391−396.
(24) Ducker, W. A.; Senden, T. J.; Pashley, R. M. *Langmuir* **1992**, *8*, 1831−1836.
(25) Hunter, R. J. *Foundation of Colloid Science*; Oxford University Press: Oxford, 2001; Vol. 2.
(26) Davis, T. A.; Llanes, F.; Volesky, B.; Mucci, A. *Environ. Sci. Technol.* **2003**, *37*, 261−267.
(27) Chibowski, S.; Mazur, E. O.; Patkowski, J. *Mater. Chem. Phys.* **2005**, *93*, 262−271.
(28) Baba, K.; Yonese, M.; Kishimoto, H. *Bull. Chem. Soc. Jpn.* **1992**, *65*, 121−128.
(29) Hook, F.; Rodahl, M.; Kasemo, B.; Brzezinski, P. *Proc. Natl. Acad. Sci. U.S.A.* **1998**, *95*, 12271−12276.
(30) Hook, F.; Rodahl, M.; Brzezinski, P.; Kasemo, B. *J. Colloid Interface Sci.* **1998**, *208*, 63−67.
(31) Haupt, B. J.; Ennis, J.; Sevick, E. M. *Langmuir* **1999**, *15*, 3886−3892.
(32) Abu-Lail, N. I.; Camesano, T. A. *J. Microsc. (Oxford, U.K.)* **2003**, *212*, 217−238.
(33) Ryden, P.; MacDougall, A. J.; Tibbits, C. W.; Ring, S. G. *Biopolymers* **2000**, *54*, 398−405.
(34) Draget, K. I.; Smidsrod, O.; Skjakbraek, G. In *Polysaccharides and Polyamides in the Food Industry. Properties, Productions, and Patents*; Rhee, A. S. a. S. K., Ed.; Wiley-VCH Verlag GmbH & Co.: Weinheim, 2005.
(35) Moe, S. T.; Skjakbraek, G.; Elgsaeter, A.; Smidsrod, O. *Macromolecules* **1993**, *26*, 3589−3597.
(36) Overbeek, J. T. G. *Prog. Biophys. Mol. Biol.* **1956**, *6*, 58−84.
(37) Lu, L.; Liu, X. X.; Dai, L.; Tong, Z. *Biomacromolecules* **2005**, *6*, 2150−2156.
(38) Draget, K. I.; Steinsvag, K.; Onsoyen, E.; Smidsrod, O. *Carbohydr. Polym.* **1998**, *35*, 1−6.
(39) Smidsrod, O.; Haug, A. *Acta Chem. Scand.* **1965**, *19*, 329−340.
(40) Qin, Y. M. *Text. Res. J.* **2005**, *75*, 165−168.
(41) Martinsen, A.; Skjakbraek, G.; Smidsrod, O. *Biotechnol. Bioeng.* **1989**, *33*, 79−89.
(42) Crist, D. R.; Crist, R. H.; Martin, J. R.; Watson, J. R. *Fems Microbiol. Rev.* **1994**, *14*, 309−313.
(43) LeRoux, M. A.; Guilak, F.; Setton, L. A. *J. Biomed. Mater. Res.* **1999**, *47*, 46−53.
(44) Chen, K. L.; Mylon, S. E.; Elimelech, M. *Environ. Sci. Technol.* **2006**, *40*, 1516−1523.

MA0527606